JOURNAL OF PROPULSION AND POWER
Vol. 19, No. 3, May–June 2003

Constant Volume Explosions of Aerosols of Metallic Mechanical Alloys and Powder Blends

Mirko Schoenitz* and Edward L. Dreizin†
New Jersey Institute of Technology, Newark, New Jersey 07102
and
Emil Shtessel‡
Exotherm Corporation, Camden, New Jersey 08103

High-energy ball milling was used to prepare sets of mechanical alloys in the systems Al–Mg, Al–Mg–H, B–Mg, and Ti–B. X-ray diffraction, electron microscopy, and low-angle laser diffraction were used to characterize structures, morphology, and sizes of the alloys, respectively. The produced materials were metastable and nanocrystalline; the particle sizes were in the range of 1–50 μm. A constant volume explosion technique was used to evaluate performance of the mechanical alloys and to compare it to the performance of blends of elemental powders of the same bulk composition. For reference, samples of mechanical alloys were annealed to produce stable intermetallic phases and tested in the same explosion experiments. Pressure traces recorded in real time served as the main piece of experimental information. After selected experiments, combustion products were collected and analyzed. The results have shown that the combustion rates of mechanical alloys are appreciably higher than those of the respective powder blends, thermodynamically stable intermetallics, and pure metals. The analyses of the combustion products also showed that combustion was more complete for mechanical alloys. It was found that combustion parameters of mechanical alloys compared to other metallic fuels were significantly improved even though their particle sizes were identical or greater than those of the reference metals. The use of mechanical alloy powders with relatively large particle sizes is expected to be advantageous in many practical applications requiring mixing and handling of energetic formulations.

Introduction

METAL additives, for example, aluminum powders, are routinely added to propellants and other energetic formulations to increase specific impulse and heat release. However, it is widely recognized that the benefits expected from metal additives are not fully exploited, mostly due to the long ignition delays and slow combustion rates of metals.

Recent research on the mechanisms of metal combustion[1–8] has shown that both ignition delay and combustion rate correlate with phase changes occurring in burning metals. Based on these results, new types of metal-based high-energy density materials have been proposed in which specific phase changes are predetermined to occur at a desired temperature and either trigger ignition or increase combustion rate of the metallic fuel. Because the desired phase change should occur rapidly, the new energetic compounds should be metastable, such as supersaturated solid solutions that include a base metal as a solvent and another component (which could be a metal or gas, such as hydrogen) as a solute, so that reaction rates would not be limited by slow solid-state diffusion processes. Such metastable solid solutions in the binary system Al–Mg have recently been prepared in laboratory quantities (tens of grams) by mechanical alloying (MA).[9,10] MA is a relatively young materials processing technique originally developed by Benjamin[11] and actively exploited in materials research and technology. Recent research in the area of new structural materials has shown that MA can be used, similar to rapid quenching, to produce highly metastable phases and supersaturated solid solutions.[12–17] Ultrafine mixing and true alloying are achieved by dry, high-energy ball milling, where an initial blend of powders is repeatedly kneaded together, cold welded and refractured by the action of ball–powder collisions.[11,12] The process usually produces a powder in which each particle has a composition nearly identical to the bulk composition of the original powder blend. Whereas detailed understanding of MA is only being developed, numerous applications have been found in metallurgy and materials processing because of its relative simplicity and efficiency.[12]

MA has not been used to prepare high energy density materials until the recent work on Al–Mg mechanical alloys.[9,10,18] In that research, ignition temperatures were investigated experimentally by using an electrically heated filament to ignite small quantities of powder. For the mechanical alloys, ignition occurred at a temperature comparable to that of pure magnesium, much lower than the temperatures required to ignite pure aluminum, for example, the $Al_{0.9}Mg_{0.1}$ mechanical alloy ignited at 1150 K, close to 1000 K for Mg, compared to 2200 K for Al. Laminar lifted aerosol flames were used in the same study to measure flame propagation rates for the combustion of the mechanical alloys in air. Here, too, flame propagation in the aerosolized alloys was nearly as fast as in pure Mg aerosols and several times faster than in aerosols of pure Al. However, a better assessment of the combustion performance of the mechanical alloys would be based on direct comparison to powder blends with the alloys' bulk compositions rather than to pure metals. This is the main objective of the present paper.

Constant volume explosions were used in this work, similar to a technique developed by the U.S. Bureau of Mines for characterization of explosibility of various dusts.[19–22] With this method, mixed powders can be handled, and therefore, a direct comparison of explosion parameters by comparing the maximum rates of pressure rise in the explosion chamber for different aerosols[21] can be made. The ability to collect the combustion products easily after each experiment for analysis is another advantage, allowing one to determine readily the completeness of the reaction. In addition to the Al–Mg mechanical alloys described earlier, mechanical alloys

Received 2 May 2002; revision received 16 December 2002; accepted for publication 16 December 2002.

*Postdoctoral Research Associate, Department of Mechanical Engineering. Member AIAA.
†Associate Professor. Member AIAA.
‡Vice President of Research and Development.

Table 1 Starting materials for mechanical alloying and combustion experiments

Material	Particle size	Purity, %	Supplier
Al (for mechanical alloys)	−100 mesh <149 μm	99.8	Atlantic Equipment Engineers
Al (for powder blends)	−325 mesh <44 μm	99.8	Atlantic Equipment Engineers
Mg (for mechanical alloys)	−50 mesh <297 μm	99+	Aldrich
Mg (for powder blends)	−325 mesh <44 μm	99.9	Aldrich
Ti (for alloys and blends)	−325 mesh <44 μm	99.7	Atlantic Equipment Engineers
B (for alloys and blends)	<1 μm (amorph.)	98.5	Atlantic Equipment Engineers
MgH_2 (for mechanical alloys)	−180 mesh <180 μm	90 (Mg)	Aldrich

in a number of different systems were prepared, characterized, and compared to their corresponding elemental powder blends.

Sample Preparation

The starting materials used in all experiments are listed in Table 1. A detailed description of the synthesis of mechanical alloys and preparation of powder blends follows.

Mechanical Alloys

A SPEX 8000 high-energy ball mill was used for preparation of the mechanical alloys in the present work. For Al–Mg and Al–MgH_2 alloys, a zirconia vial and zirconia balls were used to provide a chemically clean environment during milling. Vials and balls of stainless steel were used to prepare boron-based alloys (B–Ti and B–Mg). Batches of 10 g of each material were milled under Ar atmosphere, limited by the size of the milling vials and by safety considerations. Balls were about 10 mm in diameter, with a ball-to-powder mass ratio of 5. Size and total weight of the balls affect the required time of milling.[17] Furthermore, 2 wt% of stearic acid [CH_3–$(CH_2)_{16}$–COOH] was added during milling as a process control agent (PCA) to act against the formation of large agglomerates and to balance fracturing and cold welding in the sample powders. Milling usually raises the temperature of the sample to 50–60°C. After milling, the vials were cooled and slowly vented in air to passivate some of the powders that were pyrophoric as prepared, for example, B–Ti alloys. The powders were then dried at room temperature and under a vacuum of 600 mm Hg to remove excess PCA.

Preliminary experiments were conducted to determine the minimum time of ball milling necessary to achieve the final (steady-state) product, for example, Al with the maximum achievable amount of Mg dissolved. These experiments served to determine the final milling times for each materials system shown in Table 2.

Raw Powder Blends

In addition to mechanical alloys, blends of elemental powders with the same bulk compositions were prepared by low-energy ball milling under argon for 1 h. Alumina balls were used for this process with a ball-to-powder weight ratio of 2. Particle sizes were chosen to be comparable to the mechanically alloyed materials with the exception of boron (Table 1).

Equilibrium Alloys

The general approach followed in this study is based on the assumption that the metastable nature of the produced materials accounts for their accelerated ignition and combustion rate. Direct comparison of the combustion characteristics of the metastable mechanical alloys with those of thermodynamically stable assemblages of the same bulk composition is needed to validate this assumption. To provide such a validation, materials with the same bulk composition, particle morphologies, and most important, size distribution should be prepared to compare meaningfully their combustion characteristics. For simplicity, we annealed the metastable Al–Mg mechanical alloys at temperatures high enough to allow back-transformation to a thermodynamically stable state, but low enough to prevent significant alteration of particle size distribution or agglomeration. The temperature where spontaneous back-transformation occurs was determined using differential scanning calorimetry (DSC). A sample of the $Al_{0.7}Mg_{0.3}$ mechanical alloy was heated in a TA Instruments DSC Q-100 at 10 K/min under a 50 ml/min flow of nitrogen. The exothermic back-transformation was observed to begin at 238°C with a peak temperature of 253°C. X-ray diffraction (XRD) patterns collected from samples that were quenched before and after the transition showed that the mechanical alloys transformed to the stoichiometric intermetallic phases Al_2Mg_3 and $Al_{12}Mg_{17}$ and the equilibrium solid solution of magnesium in aluminum, respectively (discussed subsequently). Based on this information, a set of Al–Mg mechanical alloys was equilibrated for 15 min at 390°C under vacuum for use in combustion experiments.

Table 2 Milling times used to prepare mechanical alloys with a SPEX 8000 ball mill

Binary system	Milling time, h
Al–Mg	12
Al–MgH_2	21
B–Mg	12
B–Ti	3

Sample Characterization

XRD served as the main tool for phase analysis of the mechanically alloyed powders. A Philips X'pert MRD x-ray diffractometer system with Cu–Kα radiation ($\lambda = 1.5438$ Å) was used at 45 kV and 40 mA. Mechanical alloys were not ground or screened before data acquisition; powder patterns of the as-milled materials were collected. Diffraction patterns of the combustion products were collected without special preparation as well.

Particle size distributions of the mechanically alloyed powders and of their combustion products were determined by low-angle laser light scattering using a Coulter LS 230 enhanced laser diffraction particle size analyzer. Suspensions of the powders were prepared with distilled water, except for Al–Mg–H mechanical alloys and Al–Mg combustion products, where ethylene glycol [$C_2H_4(OH)_2$] was used to avoid the reaction of very fine magnesium-rich particles with water.

Al–Mg Alloys

Some of the properties of the Al–Mg mechanical alloys have been reported elsewhere[9,10]; however, a detailed description is given here to provide a complete presentation.

Crystal Structure

XRD patterns showing the evolution of the crystal structure for Al–Mg mechanical alloys with different magnesium concentrations are shown in Fig. 1. The initial Al–Mg powder blend shows sets of both Al and Mg peaks. Magnesium peaks are completely absent from the alloy diffraction patterns. With increasing Mg concentration, the peaks of aluminum shift to lower angles, which indicates an increase in the lattice parameter due to the dissolution of Mg in the Al structure. The lattice parameter increased from 4.05 Å for pure Al to 4.15 Å for the Al–30% Mg alloy. In addition, the width of the Al peaks increases indicating a significant decrease in crystallite size and an increase in lattice strain. The estimated average crystallite size, using the Scherrer equation decreased from about 0.1 μm for aluminum to about 6 nm for the alloyed powders. Whereas the equilibrium room temperature solubility of Mg in Al

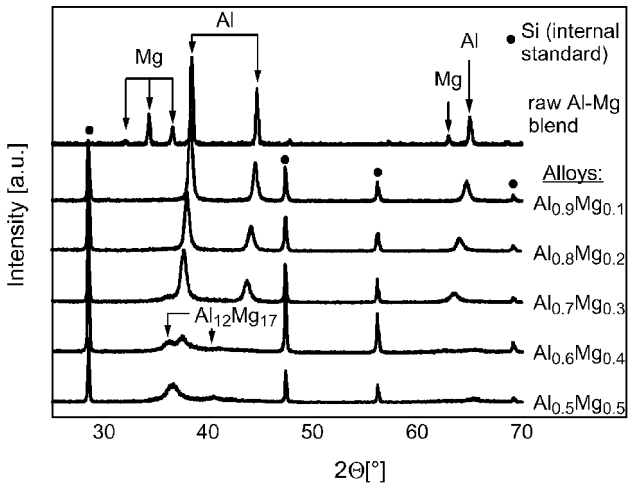

Fig. 1 X-ray patterns of an Al–Mg powder blend and Al–Mg mechanical alloys.

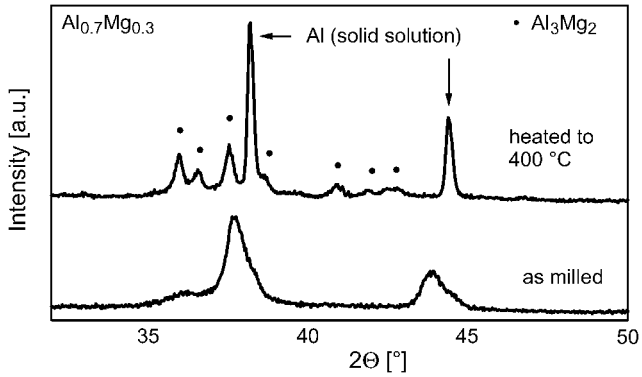

Fig. 2 XRD patterns of the $Al_{0.7}Mg_{0.3}$ mechanical alloy before and after annealing to 400°C.

does not exceed 1% (Ref. 16) up to 30% of Mg has been dissolved in the Al–Mg mechanical alloys. The mechanical alloys can, therefore, be described as metastable, nanostructured solid solutions of Mg in Al. At bulk Mg concentrations exceeding 30%, a different set of peaks is observed, consistent with the intermetallic phase $Al_{12}Mg_{17}$ (Refs. 23 and 24).

XRD patterns of the $Al_{0.7}Mg_{0.3}$ alloy before and after annealing are shown in Fig. 2. The peaks of the Al solid solution in the pattern of the annealed alloy are shifted back to their equilibrium positions. Peaks sharpened as a result of increased crystallite size and reduced lattice strain. The stoichiometric equilibrium phase Al_3Mg_2 (marked peaks in Fig. 2) (Refs. 23 and 24) formed during annealing.

Particle Sizes

Results are shown in Fig. 3 for the $Al_{0.7}Mg_{0.3}$ mechanical alloy. The particle size of the Al-Mg mechanical alloys varies little with magnesium concentration. The mechanically alloyed powders have fairly wide size distributions with mean particle sizes (volume averages) generally larger than for the pure magnesium and aluminum powders used in the reference powder blends. The averages indicated ($\langle d \rangle$) are volume mean diameters. Size distribution of the other mechanical alloys closely resemble the example shown in Fig. 3. Particle shapes, as determined independently from electron micrographs, were irregular, but generally close to spherical. Note that the size of the mechanically alloyed powders can be controlled by the size of the balls used during milling and by the type and amount of the process control agent[17]; however, because of the limited time and scope of the present effort no such adjustments have been made.

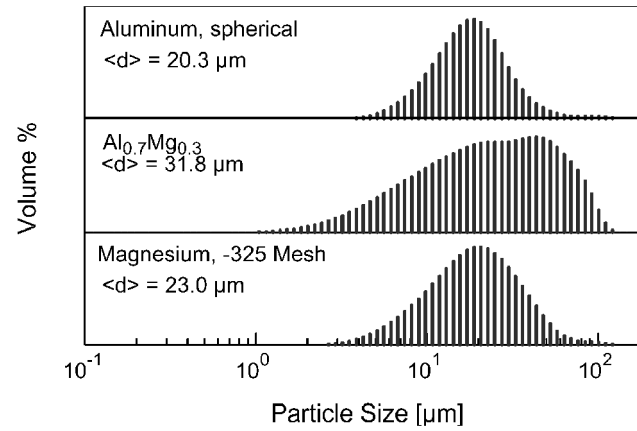

Fig. 3 Particle size distributions of the $Al_{0.7}Mg_{0.3}$ mechanical alloy powder and aluminum and magnesium powders used to prepare reference powder blends.

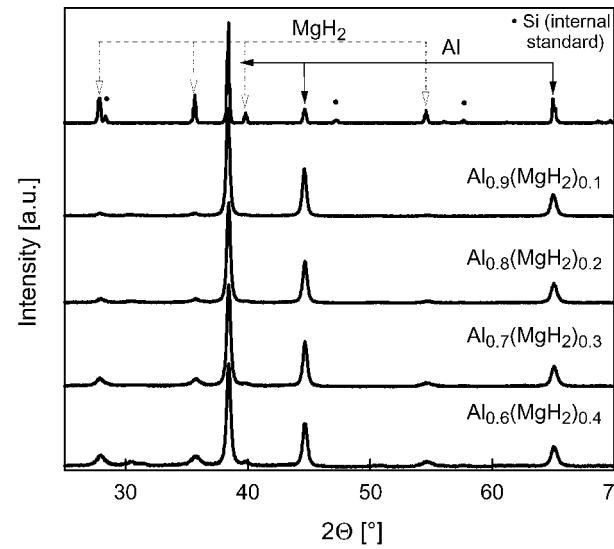

Fig. 4 X-ray patterns of the raw powder blend and mechanical alloys in the Mg–Al–H system.

Al–Mg–H Alloys

Crystal Structure

The XRD patterns of the Al–MgH_2 alloys are shown in Fig. 4. The intensities of the MgH_2 peaks significantly decreased after ball milling, but they do not completely disappear. Peak widths for both, Al and MgH_2 increase, which indicates decreasing crystallite sizes and increasing lattice strain. However, the Al peak positions barely shift, in contrast to the quite substantial peak shifts observed for the Al–Mg mechanical alloys. In this system, and under the present milling conditions, Mg, or MgH_2 appears not to dissolve into the aluminum structure to the degree observed in the Al–Mg system. This indicates that the Al–Mg–H mechanical alloys have a different structure than the Al–Mg alloys. Further analyses are needed to elucidate the differences in the mechanisms of formation of these two types of aluminum-based mechanical alloys.

Particle Sizes

Particle size distributions for the Al–Mg–H mechanical alloys are comparable to the particle size distributions of the Al–Mg alloys described earlier. Mean particle sizes vary from 30 to 40 μm.

B–Ti Alloys

Crystal Structure

The boride formation reactions $B + Ti \rightarrow TiB$ and $2B + Ti \rightarrow TiB_2$ were expected to present a major challenge to the synthesis

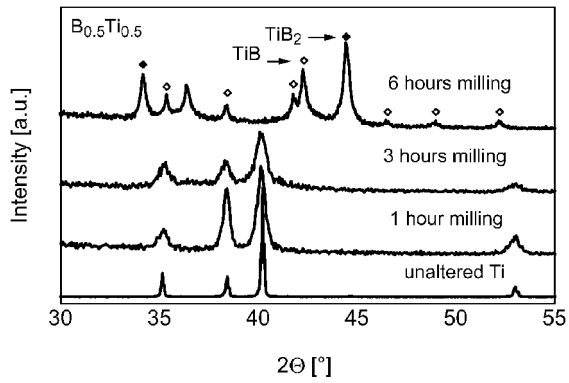

Fig. 5 X-ray patterns of the B–Ti powder blend and a series of $B_{0.5}Ti_{0.5}$ mechanical alloys prepared during different milling times.

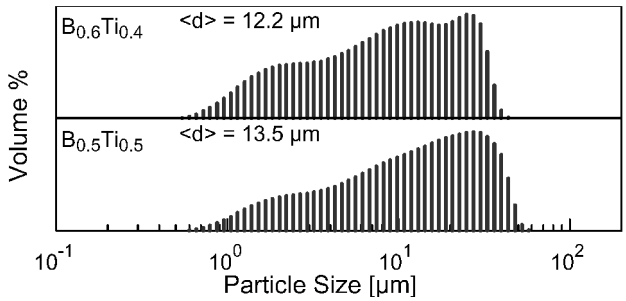

Fig. 6 Size distributions of B–Ti mechanical alloy powders; mean particle sizes labeled as $\langle d \rangle$.

of B–Ti mechanical alloys. Therefore, detailed observations of the changes in the powder structures were conducted in short intervals over the total time of milling.

Figure 5 shows that the formation of TiB and TiB_2 occurred after a relatively short milling time for the compositions of $B_{0.6}Ti_{0.4}$, and $B_{0.5}Ti_{0.5}$. Initially, the titanium peaks widen, and after only a short time of continued milling, spontaneous, and nearly complete formation of borides occurs, accompanied by a large exothermic effect. The exact time of transformation varies somewhat from one batch to another, depending on minute variations in milling conditions, but was generally observed after 3–4 h. Boride formation occurred much more gradually for lower Ti concentrations. The first TiB_2 peaks were observed after 9 h of milling, and boride and unreacted titanium were simultaneously present in the mechanical alloy.

Because titanium boride powders are not reactive in oxidizing environments, alloying was interrupted just before their formation. The $B_{0.6}Ti_{0.4}$ and $B_{0.5}Ti_{0.5}$ mechanical alloys thus prepared were pyrophoric and reacted violently when initiated mechanically or thermally. Once ignited, such powders self-dispersed and produced a burning aerosol cloud.

Particle Sizes

Even though the initial boron powder used in preparation of mechanical alloys was extremely fine, the B–Ti mechanical alloy powders had sizes in the 10-μm range (Fig. 6). Electron micrographs showed the alloy powders to be nearly spherical. Therefore, handling procedures for such powders relevant to energetic formulations are expected to be much simpler than for pure ultrafine boron powders.

B–Mg Alloys

One sample of a $B_{0.5}Mg_{0.5}$ mechanical alloy was prepared. The XRD patterns for this material shows that crystallite sizes decrease, but otherwise no fundamental changes occur after prolonged times of milling. No boride phases were observed in these alloys. The particle size distribution is relatively wide with a mean size of 23 μm. As in the case of B–Ti alloys, the particle size of the mechanical alloy does not reflect the particle size of the original B powder.

Constant Volume Explosion Experiments

The explosion apparatus was designed on the basis of the U.S. Bureau of Mines setup[19–22]; a schematic diagram is shown in Fig. 7. The constant volume vessel, or explosion chamber was constructed of two schedule-40-type304 stainless steel 40-cm i.d. welding caps. The two halves are held together by four equally spaced external clamps and sealed with an O-ring. The vessel volume is 9.2 liter. A particle dispersion nozzle is positioned in the center of the bottom half of the chamber over the gas (air) inlet. The bottom half of this chamber has ports for the pressure transducer and a vacuum line. The upper half of the chamber has electrical feedthroughs for the igniter.

The explosion chamber is connected through a 15-mm i.d. solenoid valve to a 7.6-liter reservoir tank, which was pressurized to about 6 atm with commercial grade dry compressed air for dispersing the dust. (All reported pressures are absolute values). The solenoid valve was used to admit a short pulse of air to the explosion chamber, dispersing the powder through the nozzle and raising the chamber pressure to approximately 0.8 atm. The solenoid valve operation and subsequent electrical initiation of the igniter was controlled by relays connected to the output of an electronic controller. In the experiments, metal powder was loaded into a pipe elbow under the dispersion nozzle, the explosion chamber sealed and evacuated to 0.2 atm, the reservoir air tank pressurized, and the electronic controller tripped. The controller initiates the data acquisition system (discussed later), then provides a 0.2-s pulse to admit the air (solenoid valve) and, after a delay of 0.3 s, provides a pulse to activate the igniter. The delay time of 0.3 s was chosen to reduce the level of turbulence in the chamber while minimizing gravitational settling of the dispersed powder.

A hot-wire igniter was made of a 5-cm-long tungsten wire with a diameter of 100 μm. The duration of the ignition pulse was 60 ms, the voltage used was 23 V AC, and the current was 3.5 A. Thus, the total energy released by the ignition pulse was about 5 J, much less than the 500, 1000, or 2500 J per igniter typically used in similar experiments by the U.S. Bureau of Mines researchers.[20] Combustion of tungsten itself is relatively slow, and ignition of the sample charge most likely occurred by contact with the electrically heated wire before its oxidation. Subsequent combustion of the igniter could have contributed up to 80–100 J to the total heat released by the explosion. The effect of the igniter on recorded pressure traces could not be detected in test experiments that were conducted with identical parameters but without dispersed powders.

The dispersion nozzle was constructed according to the design used in the 20-liter Bureau of Mines chamber.[19] The hemispherical nozzle has three rows of cylindrical holes positioned radially. The sizes of the nozzle and the holes were scaled for the 9.2 liter chamber using Bureau of Mines design drawing dimensions to provide the same estimated gas speed when passing through the nozzle.

A strain gauge with a full range of 20 atm monitored the chamber pressure. The transducer response time is about 0.002 s for full-scale

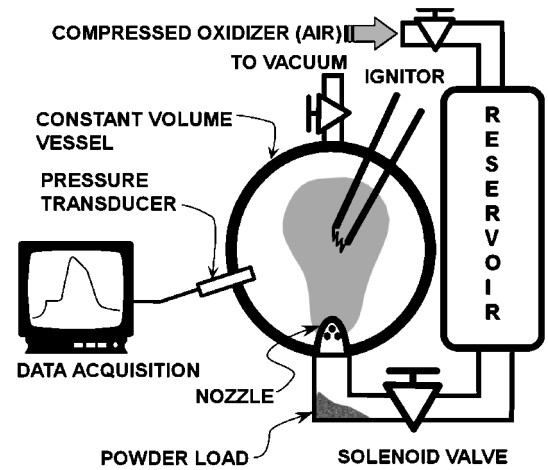

Fig. 7 Schematic diagram of the constant volume explosion apparatus.

deflection and it has a rated accuracy of ±0.2% of full scale. The transducer is housed in a 1.2-cm i.d. pipe threaded to the chamber. The output from the pressure transducer and the time reference pulses from an electronic sequencer were stored on a personal computer using a OS-220 Scope Lab Card (Hung Chang Co.)

All explosion experiments were conducted targeting an equivalence ratio of 1.5. The corresponding nominal dust concentrations range from 480 (Al) to 550 ($Al_{0.5}Mg_{0.5}$) to 650 g/m^3 (Mg) and from 190 (B) to 450 g/m^3 ($B_{0.5}Ti_{0.5}$).

Results and Discussion

A number of parameters can be determined and compared as a result of constant volume explosion experiments, including the rate of pressure rise, ratio of the maximum to the initial explosion pressures, ignition delay time, ignition energy, flame propagation and extinction times, final pressure and gas composition in the vessel after explosion, morphology and composition of the condensed combustion product, and other parameters, such as radiation intensity. Each of these measurements is useful in elucidating the combustion mechanism. However, note that the interpretation of many of these measurements is not straightforward because of the complex nature of the processes occurring during explosion in a constant volume vessel. Because of the limited scope of this work aimed primarily at the comparison of combustion performance of different materials, the emphasis was placed on the measurements of the rate of pressure rise as the single most important characteristic of combustion in this type of experiment. In addition, condensed combustion products were collected and analyzed.

Mg–Al and Al–Mg–H Systems

The experimental results on explosion of Al–Mg mechanical alloys and powder blends are shown in Figs. 8–10. Figure 8 shows a series of the pressure traces measured during explosions of Al–Mg mechanical alloys and powder blends with identical bulk compositions. All fuel–air mixtures shown in Fig. 8 were ignited at $t = 0.5$ s. Figure 9 shows the corresponding rates of pressure rise. Before the summary presented in Fig. 10 is discussed, note that some inconsistency in ignition delays was observed. This inconsistency could not be presently interpreted because different ignition delays could be caused by either difference in the particle size distribution or by inconsistency in the operation of the ignition circuit. Further improvements of the experimental setup are planned to address the issue in future work.

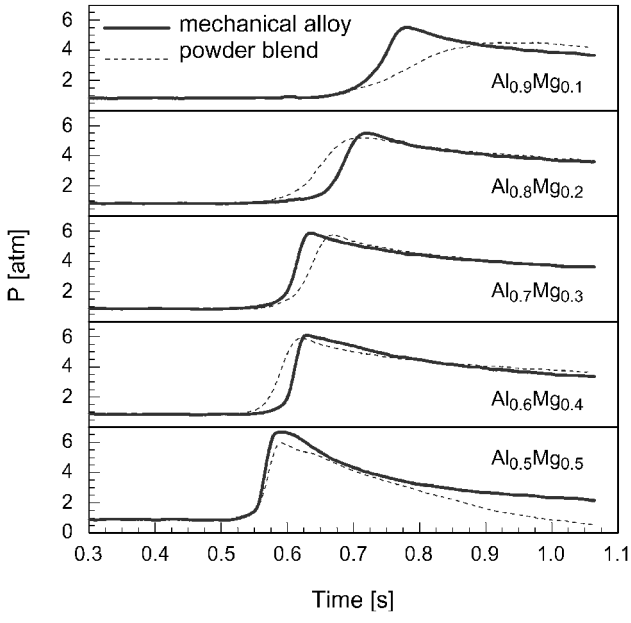

Fig. 8 Pressure traces of constant volume explosions of fuel–air mixtures with different Al–Mg powder blends and mechanical alloys as fuels. The fuel–air mixtures were ignited at $t = 0.5$ s.

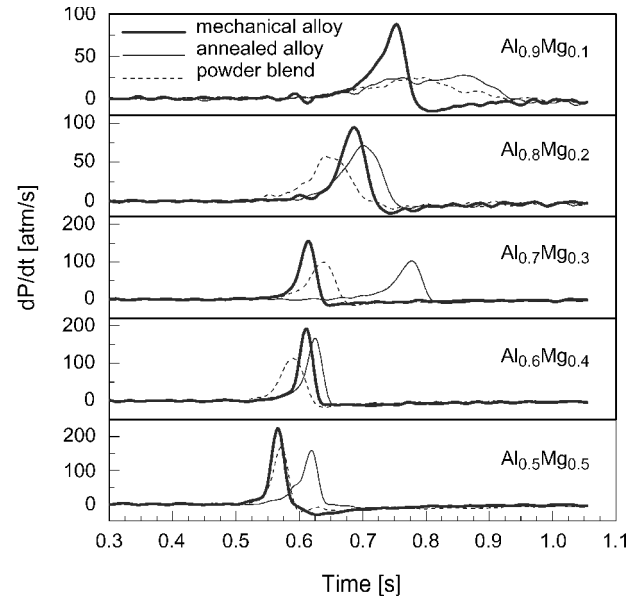

Fig. 9 Time derivatives of the pressure traces of constant volume explosion experiments for the Al–Mg mechanical alloys. Traces for annealed alloys and powder blends are shown for comparision.

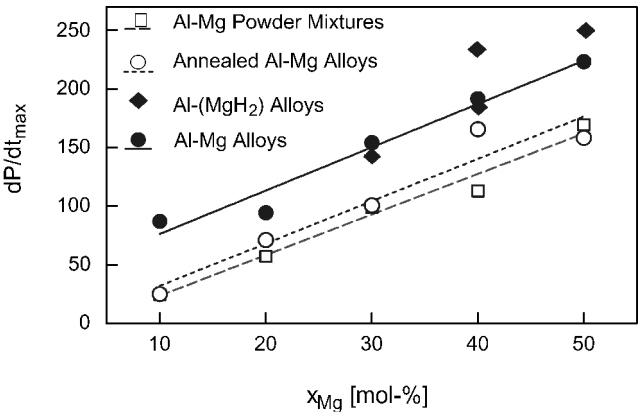

Fig. 10 Summary of measurements on the maximum value of the derivative dP/dt_{max} for constant volume explosions of fuel–air mixtures with different Al–Mg and Al–Mg–H mechanical alloys and powder blends as fuels.

It can be clearly seen from Figs. 9 and 10 that the alloys consistently outperform mechanical powder blends and thermodynamically stable alloys in their maximum rate of pressure rise dP/dt_{max}. The higher maximum pressures observed in the experiments with mechanical alloys also indicate a more complete combustion because the overall enthalpies of reaction are essentially the same for alloys and the respective metal powder blends. The similarity of enthalpies was confirmed earlier by measurements with an oxygen bomb calorimeter.[18] Note that the absolute values of the pressures and rates of pressure rise determined in these experiments cannot be directly compared with similar values reported in earlier work using a similar experimental technique. To provide a valid comparison, the igniter energy, initial gas pressure, and the vessel shape and size must be exactly the same. However, as already mentioned, the ignition energies used were several orders of magnitude lower than those of chemical igniters used in earlier work.[19–21] In addition, the initial gas pressure was consistently maintained to be less than 1 atm (close to 0.8 atm) to limit the maximum explosion pressure while working with some of the new and highly reactive materials.

As noted, in this research we focus on the comparisons of the values of $(dP/dt)_{max}$, which characterizes the maximum flame propagation rate.[25] This parameter is a function of the vessel size, igniter energy, and initial conditions, all of which were maintained constant.

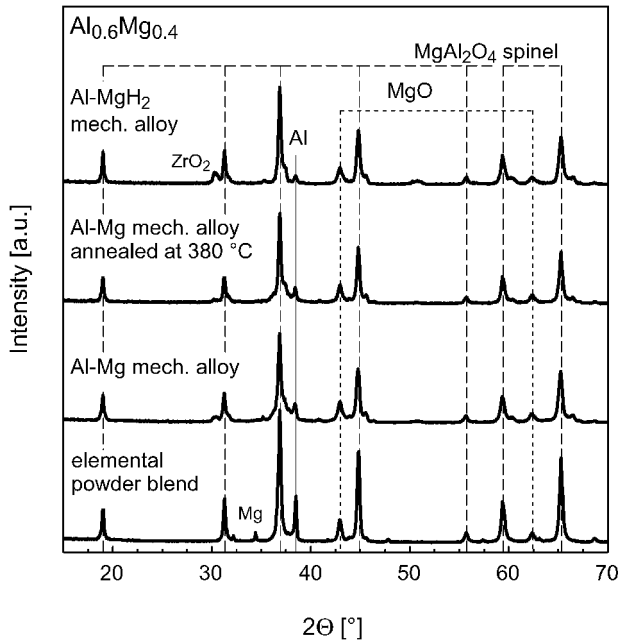

Fig. 11 XRD patterns for the combustion products of the elemental powder blend, mechanical alloy, annealed alloy, and the mechanical alloy produced in the Al–MgH_2 system for compositions with 60 mol-% Al.

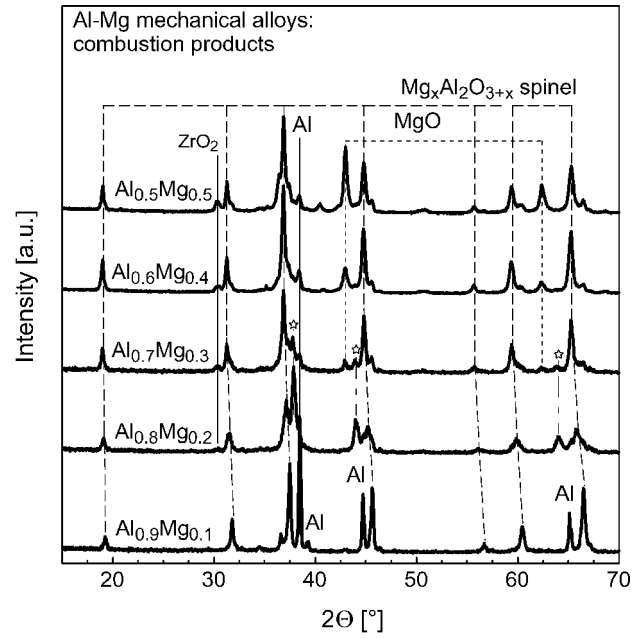

Fig. 12 Comparison of XRD patterns for the combustion products of mechanical alloys in the Al–Mg system; unmarked peaks are Mg and Al–Mg intermetallic phases.

It depends much less on the complex flame propagation processes occurring in the bomb than some other experimental parameters, and it is a usual practice to compare the constant volume explosion experiments based on this quantity.[19–21]

A summary of the experimental results on Al–Mg and Al–Mg–H mechanical alloy systems is given in Fig. 10. Linear fits for the data sets are also shown. The experimental results on $(dP/dt)_{max}$ are compared for the metastable mechanical alloys, annealed mechanical alloys that have the same particle sizes and bulk composition, but consist of phases in thermodynamic equilibrium, and Al–Mg–H mechanical alloys. The comparison shows that both Al–Mg and Al–Mg–H metastable mechanical alloys produce a higher rate of pressure rise and, thus, a faster propagating combustion wave than powder blends or equilibrium alloys of the same composition. Very high rates of pressure rise are observed for the Al–Mg–H alloys with higher MgH_2 contents and the differences in the combustion mechanisms of these materials compared to the Al–Mg alloys will be addressed in future work.

Combustion products were collected after all experiments, and selected samples were analyzed by XRD. Some XRD patterns for combustion products for the Al–Mg powder blends and mechanical alloys are presented in Figs. 11 and 12. The XRD patterns show that Al_2MgO_4 spinel is the main combustion product for all Al–Mg powder blends and Al–Mg, and Al–MgH_2 mechanical alloys. Figure 11 shows representative diffraction patterns for materials with 60 mol-% Al. The mechanical alloys and the annealed alloys are very similar, and the higher intensity of the main Al peak shows that combustion in the case of the powder blend was less complete. The diffraction patterns shown in Fig. 12 for Al–Mg mechanical alloys with varying compositions exhibit noticeable peak shifts, indicating varying stoichiometry and defect concentration of the spinel phase. The x-ray patterns further show peaks of unreacted Al and Mg, especially in the patterns of the combustion products of powder blends. Generally, based on the comparison of relative peak intensities, it appears that smaller quantities of the unreacted material are present in the combustion products of mechanical alloys than in those of powder blends. Note that peaks consistent with a nitride phase (aluminum nitride, AlN; Powder Diffraction File,[25] reference identification number 25-1495) are observed for the combustion products of the $Al_{0.7}Mg_{0.3}$ and $Al_{0.8}Mg_{0.2}$ mechanical alloys (peaks marked with stars in Fig. 12). The peaks of unreacted aluminum nearly disappear from the x-ray patterns of these products, but become stronger again in the combustion products of the $Al_{0.9}Mg_{0.1}$ or $Al_{0.6}Mg_{0.4}$ alloys. This suggests the possibility that in the experiments with 20 and 30% of magnesium, sufficient amounts of hot and reactive aluminum remain after the oxygen is consumed and this aluminum further reacts with nitrogen. The ZrO_2 contamination shown in Fig. 12 indicates detritus from the milling vial.

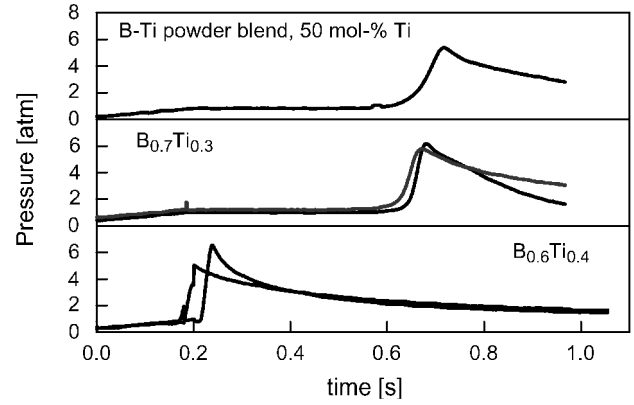

Fig. 13 Selected pressure traces of constant volume explosions of fuel–air mixtures with different B–Ti mechanical alloys and a 50% Ti powder blend as fuels.

B–Ti System

A selection of pressure traces for the B–Ti system is shown in Fig. 13. Multiple traces indicate experiments with the same powders. Powder blends were prepared for the same bulk compositions as the mechanical alloys; however, only the blend with 50 at.% of titanium could be ignited with the igniter used. At the same time, all of the prepared mechanical alloys (with 10, 20, 30, 40, and 50 at.% of titanium) were successfully ignited with the same igniter energies, even though combustion of the alloy with 10 at.% of titanium was quite slow. As already noted, the mechanical alloys with 40 and 50 at.% of titanium were pyrophoric and were observed to ignite in these experiments as a result of the pressure blast rather than the regular hot-wire igniter. That is, these two types of the alloy powders ignited before the hot-wire igniter was energized, as indicated by the pressure traces shown in Fig. 13.

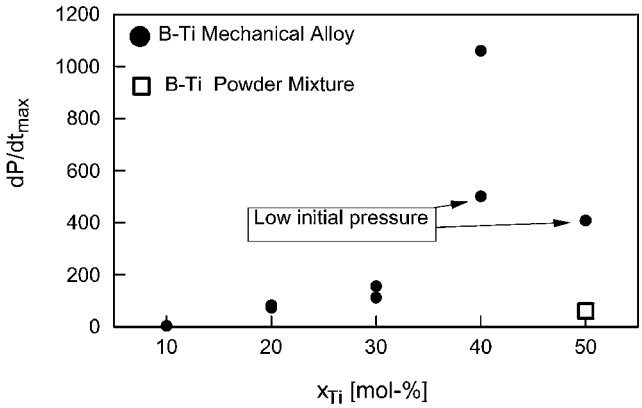

Fig. 14 Summary of the maximum value of the pressure derivative dP/dt_{max} for constant volume explosions of fuel–air mixtures with different B–Ti mechanical alloys and powder blends as fuels. The igniter was fired at $t = 0.5$ s in all experiments.

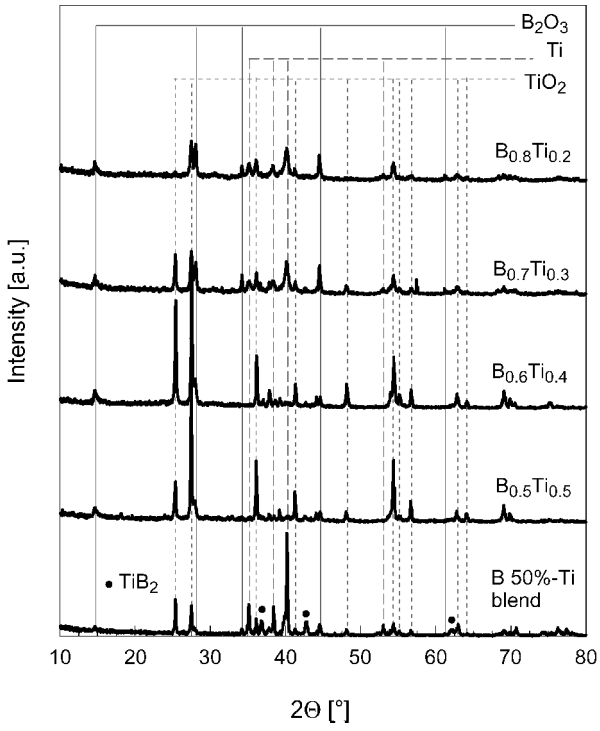

Fig. 15 XRD patterns for combustion products of B–Ti mechanical alloys and a power blend with 50 mol-% of Ti.

The values of dP/dt_{max} are summarized in Fig. 14. Rates of pressure rise were very fast for these pyrophoric mechanical alloys. The smaller values of dP/dt_{max} observed for the $B_{0.5}Ti_{0.5}$ alloy, compared to the $B_{0.6}Ti_{0.4}$ alloy, could be because the ignition occurred during the pressure blast and, therefore, at a significantly lower initial chamber pressure.

Combustion products of the experiments with the B–Ti powder blend (50% Ti) and $B_{0.5}Ti_{0.5}$ and $B_{0.6}Ti_{0.4}$ alloys were collected and analyzed by XRD. The results are shown in Fig. 15. The products of the powder blend contain significant amounts of unreacted titanium and some TiB_2 in addition to the boron and titanium oxides. Note that no appreciable titanium boride peaks are observed in the combustion products of mechanical alloys. These consist essentially of a mixture of titanium and boron oxides. Therefore, the completeness of oxidation for the B–Ti mechanical alloys is much greater than that for powder blends of the same composition. This is a significant conclusion; further analyses of phase changes occurring during combustion of mechanical alloys in the B–Ti system are clearly warranted. Preliminary considerations indicate that the two types of reactions, oxidation and intermetallic Ti–B

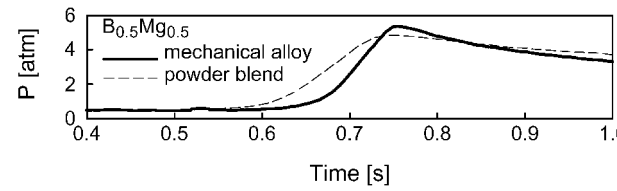

Fig. 16 Pressure traces of constant volume explosions of B-Mg fuel–air mixtures.

reaction, occur simultaneously in the Ti–B system. Formation of Ti–B compounds is likely to occur faster in the mechanical alloys than in powder blends, and titanium borides are less reactive with oxygen than pure B or Ti. Consequently, the rapid formation of less combustible Ti–B compounds during the explosion was expected to prevent complete oxidation. However, observed reaction rates and the completeness of combustion were higher for mechanical alloys and lower for the powder blend. This suggests that, in mechanical alloys where Ti–B reactions are not limited by diffusion, these reactions are rapid enough to occur nearly adiabatically. Thus, the newly formed Ti–B compounds are heated to very high temperatures where their complete oxidation is possible. Therefore, mechanical alloys enable one to increase significantly the overall combustion enthalpy in the Ti–B systems by releasing both intermetallic reaction and oxidation enthalpies at the same time.

B–Mg System

Only one composition (with 50 mol-% of boron) was prepared for this material. The experiments on ignition of the B–Mg alloy were successful, and both alloy and powder blend explosion tests were conducted. The results of these experiments are shown in Fig. 16. The aerosol was ignited $t = 0.5$ s. It was observed that both maximum pressure and the rate of pressure rise are higher for the B–Mg mechanical alloy than for a powder blend with the same bulk composition. Additional experimental work is needed for a more detailed characterization of B–Mg mechanical alloys.

Conclusions

The results of this work are preliminary because of its limited scope; however, it was clearly shown that different types of mechanical alloy powders could be prepared and used to improve significantly combustion and explosion parameters of energetic formulations.

The results of the closed vessel explosion experiments in the Al–Mg system showed that the metastable mechanical alloys exhibited higher rates of combustion and a more complete oxidation than either pure powder blends of the same composition or equilibrium intermetallic phases. An additional increase in the combustion rate and pressure was achieved for Al–Mg–H mechanical alloys. The comparison of explosion parameters and combustion products of the metastable Al–Mg mechanical alloys and pure aluminum powders of different sizes showed that much faster combustion rates, higher explosion pressures, and a more complete oxidation could be achieved with mechanical alloys. These improved combustion parameters combined with the relatively large particle sizes of mechanical alloy powders produce a combination that appears very attractive for practical applications: highly energetic, readily ignitable materials that burn completely and are easy to handle and mix.

For the B–Ti system, the feasibility of metastable and highly reactive Ti–B mechanical alloys was demonstrated. Qualitative improvements in the ignitability of boron powders mechanically alloyed with titanium were observed, compared to pure boron powders. The closed-vessel explosion tests showed that very high combustion rates and that completeness of boron and titanium oxidation could be achieved when metastable B–Ti alloys were used as fuels. It was also found that the main combustion products of the B–Ti alloys are boron and titanium oxide phases, whereas significant amounts of TiB_2 were observed to form in the combustion products of a blend of boron and titanium powders. Whereas pure boron has been ignited in similar experiments using igniters with much

higher energy [2500 J (Ref. 22)], successful ignition with low energies in the present study (<100 J) emphasizes that significant improvements in the boron combustion and ignition parameters were achieved using relatively coarse mechanical alloy powders. The issue of the observed pyrophoricity of some of the produced B–Ti alloys needs to be addressed in future work.

Preliminary results have also shown an improvement in the boron reactivity for the prepared B–Mg mechanical alloys.

In summary, improvements in explosion rate of pressure rise and completeness of the oxidation are observed for a range of mechanical alloys and further work is needed to provide a more detailed characterization and description of the mechanical alloy combustion mechanisms. It is also necessary to address development and the scaleup of the mechanical alloying powder processing for transition to practical applications.

Acknowledgments

This work was primarily supported by the Defense Threat Reduction Agency, Contract 01-01-9-0158, monitored by Kibong Kim and by the Office of Naval Research, Grant N00014-00-1-0446, monitored by Judah Goldwasser. Additional support was provided by the New Jersey Commission on Science and Technology, Award 01-2042-007-24. The comments of two anonymous reviewers were helpful and are greatly appreciated.

References

[1]Dreizin, E. L., "Experimental Study of Stages in Aluminum Particle Combustion in Air," *Combustion and Flame*, Vol. 105, No. 4, 1996, pp. 541–556.

[2]Dreizin, E. L., Keil, D. G., Felder, W., and Vicenzi, E. P. "On the Mechanism of Boron Ignition" *1997 JANNAF Combustion Subcommittee, Propulsion Systems Hazards Subcommittee and Airbreathing Propulsion Subcommittee Joint Meeting*, 1997.

[3]Molodetsky, I. E., Dreizin, E. L., Vicenzi, E. P., and Law, C. K., "Phases of Titanium Combustion in Air" *Combustion and Flame*, Vol. 112, No. 4, 1998, pp. 522–532.

[4]Dreizin, E. L., "Experimental Study of Aluminum Particle Flame Evolution in Normal and Micro-Gravity," *Combustion and Flame*, Vol. 116, No. 3, 1999, pp. 323–333.

[5]Molodetsky, I. E., Dreizin, E. L., and Law, C. K., "Evolution of Particle Temperature and Internal Composition for Zirconium Burning in Air," *Twenty-Sixth Symposium (International) on Combustion*, Combustion Inst., Pittsburgh, PA, 1997, pp. 1919–1927.

[6]Dreizin, E. L., "On the Mechanism of Asymmetric Aluminum Particle Combustion," *Combustion and Flame*, Vol. 117, No. 4, 1999, pp. 841–850.

[7]Dreizin, E. L., Keil, D. G., Felder, W., and Vicenzi, E. P., "Phase Changes in Boron Ignition and Combustion," *Combustion and Flame*, Vol. 119, No. 3, 1999, pp. 272–290.

[8]Dreizin, E. L., "Phase Changes in Metal Combustion" *Progress in Energy and Combustion Science*, Vol. 26, No. 1, 2000, pp. 57–78.

[9]Shoshin, Y. L., Mudryy, R., and Dreizin, E. L., "Preparation of Al–Mg Mechanical Alloys and Testing Their Ignition and Combustion Parameters," *Proceedings of the 2nd Joint Meeting of the U.S. Sections of the Combustion Institute* (submitted for publication).

[10]Shoshin, Y. L., Mudryy, R. S., and Dreizin, E. L., "Preparation and Characterization of Energetic Al–Mg Mechanical Alloy Powders," *Combustion and Flame*, Vol. 128, No. 3, 2002, pp. 259–269.

[11]Benjamin, J. S., "Mechanical Alloying—A Perspective," *Metal Powder Report*, Vol. 45, Feb. 1990, pp. 122–127.

[12]Suryanarayana, C. (ed.), *Non-Equilibrium Processing of Materials*, Pergamon, Amsterdam, 1999.

[13]Wen, C. E., Kobayashi, K., Sugiyama, A., Nishio, T., and Matsumoto, A., "Synthesis of Nanocrystallite by Mechanical Alloying and In Situ Observation of Their Combustion Phase Transformation in Al_3Ti," *Journal of Materials Science*, Vol. 35, No. 8, 2000, pp. 2099–2105.

[14]Nebti, S., Hamana, D., and Cizeron, G., "Calorimetric Study of Pre-Precipitation and Precipitation in Al-Mg alloy," *Acta Metallurgica et Materialia*, Vol. 43, 1995, pp. 3583–3588.

[15]Lu, L., and Zhang, Y. F., "Influence of Process Control Agent on Interdiffusion Between Al and Mg During Mechanical Alloying," *Journal of Alloys and Compounds*, Vol. 290, Nos. 1/2, 1999, pp. 279–283.

[16]Clark, C. R., Suryanarayana, C., and Froes, F. H., "Solid Solubility Extension in Lightweight Alloys by Mechanical Alloying" in "Synthesis/Processing of Lightweight Metallic Materials," edited by F. H. Froes, C. Suryanarayana, and C. M. Ward-Close, Minerals, Metals and Materials Society, 1995, pp. 175–182.

[17]Suryanarayana, C., "Mechanical Alloying and Milling," *Progress in Materials Science*, Vol. 46, Nos. 1/2, Jan. 2001, pp. 1–184.

[18]Dreizin, E., Shoshin, Y., and Mudryy, R., "High Energy Density Powders of the Al–Mg Mechanical Alloys," *50th JANNAF Joint Propulsion Meeting*, 2001.

[19]Hertzberg, M., Cashdollar, K. L., and Opferman, J. J., "The Flammability of Coal Dust–Air Mixtures," U.S. Bureau of Mines, Rept. RI8360, 1979.

[20]Cashdollar, K. L., and Hertzberg, M., "20-l Explosibility Test Chamber for Dusts and Gases," *Review of Scientific Instruments*, Vol. 56, No. 4, April 1985, pp. 596–602.

[21]Cashdollar, K. L., and Chatrathi, K., "Minimum Explosible Dust Concentrations Measured in 20-L and 1-m^3 Chambers," *Combustion Science and Technology*, Vol. 87, 1992, p. 157.

[22]Cashdollar, K. L., "Flammability of Metals and Other Elemental Dust Clouds," *Process Safety Progress*, Vol. 13, 1994, pp. 139–145.

[23]Massalski, T. B., Okamoto, H., Subramanian, P. R., and Kacprzak, L. (eds.), *Binary Alloy Phase Diagrams*, ASM Publications, Materials Park, OH, 1990.

[24]Lewis, B., and von Elbe, G., *Combustion, Flames and Explosions of Gases*, Academic Press, New York, 1987, p. 388.

[25]"Powder Diffraction File (PDF-2)," Joint Committee for Powder Diffraction Standards—International Center for Diffraction Data, Newton Square, PA, 1988.